

**Construction of a model for the improved planning  
of MCO-informed VMAT in RayStation using a  
knowledge base of clinical IMRT-MCO treatment  
plans**

by

Caroline M. Colbert

Submitted to the Department of Nuclear Science and Engineering  
in partial fulfillment of the requirements for the degree of  
Bachelor of Science in Nuclear Science and Engineering  
at the

MASSACHUSETTS INSTITUTE OF TECHNOLOGY

June 2017

© Massachusetts Institute of Technology 2017. All rights reserved.

Author .....  
Department of Nuclear Science and Engineering  
May 18, 2017

Certified by .....  
Michael P. Short  
Assistant Professor of Nuclear Science and Engineering  
Thesis Supervisor

Accepted by .....  
Michael P. Short  
Assistant Professor of Nuclear Science and Engineering,  
Undergraduate Chair



**Construction of a model for the improved planning of  
MCO-informed VMAT in RayStation using a knowledge  
base of clinical IMRT-MCO treatment plans**

by

Caroline M. Colbert

Submitted to the Department of Nuclear Science and Engineering  
on May 18, 2017, in partial fulfillment of the  
requirements for the degree of  
Bachelor of Science in Nuclear Science and Engineering

**Abstract**

Intensity Modulated Radiation Therapy (IMRT) is a type of external beam radiation therapy that has proven effective at treating many cancers. A related therapy type, Volumetric Modulated Arc Therapy (VMAT), has the potential to provide comparable dose coverage to tumor sites while better sparing nearby organs at risk (OARs). Multi-criteria Optimization (MCO) is an algorithm that is used to optimize a patient's personalized IMRT treatment plan. VMAT treatment plans cannot be optimized using early versions of the MCO algorithm. The purpose of this study was to construct a model for the automated generation of VMAT treatment plans for prostate cancers using a knowledge base of previously implemented IMRT-MCO treatment plans. An initial model configuration was iteratively refined to produce VMAT plans that represent a quality "first pass" that can be further optimized by trained treatment planners. The clinical implementation of a model like this one could significantly improve the timeliness of standard non-MCO VMAT optimization methods.

Thesis Supervisor: Michael P. Short

Title: Assistant Professor of Nuclear Science and Engineering



## Acknowledgments

I would like to thank Professor Michael Short of the Department of Nuclear Science and Engineering for his guidance during this project and his support of my pursuit of this unique research opportunity. In addition, I am particularly indebted to Michael Young of the department of Radiation Oncology and Medical Physics at the Massachusetts General Hospital for providing me with the opportunity to contribute to this research. The mentorship I have received over the course of this and our other projects has been of immense value. I am fortunate to have found a mentor so willing to create opportunities for me.



# Contents

|   |           |
|---|-----------|
| <b>Contents</b>                                   | <b>7</b>  |
| <b>List of Figures</b>                            | <b>9</b>  |
| <b>List of Tables</b>                             | <b>11</b> |
| <b>1 Introduction</b>                             | <b>13</b> |
| <b>2 Background</b>                               | <b>17</b> |
| 2.1 History of Modern Radiation Therapy . . . . . | 17        |
| 2.2 IMRT and VMAT . . . . .                       | 18        |
| 2.3 The Dose-Volume Histogram . . . . .           | 21        |
| 2.4 Multi-Criteria Optimization . . . . .         | 22        |
| 2.5 MCO-Informed VMAT . . . . .                   | 23        |
| <b>3 Methods</b>                                  | <b>27</b> |
| 3.1 Patient Cohort . . . . .                      | 27        |
| 3.2 Knowledge Base Construction . . . . .         | 27        |
| 3.3 Model Construction . . . . .                  | 28        |
| <b>4 Results and Discussion</b>                   | <b>33</b> |
| 4.1 Knowledge Base . . . . .                      | 33        |
| 4.2 Automated Treatment Planning Model . . . . .  | 34        |

|          |                                     |           |
|----------|-------------------------------------|-----------|
| 4.3      | Limitations of this Study . . . . . | 38        |
| <b>5</b> | <b>Conclusion</b>                   | <b>39</b> |
| <b>A</b> | <b>Regions of Interest</b>          | <b>43</b> |
| <b>B</b> | <b>DVH Data Cleaning Script</b>     | <b>45</b> |
|          | <b>Bibliography</b>                 | <b>51</b> |



# List of Figures

|     |   |    |
|-----|---|----|
| 2-1 | The first patient treated with a medical linear accelerator was a two-year-old boy with an ocular tumor [1]. . . . .  | 18 |
| 2-2 | A typical MLC consists of 40 pairs of tungsten “leaves” that are independently driven. MLCs are ideal for treatment modalities like IMRT and VMAT that utilize many beam shapes and modulated beam intensity [2]. . . . .   | 19 |
| 2-3 | Archetypal case of a target volume (red) wrapped around an OAR (green). Simply “blocking” dose from reaching the OAR does not achieve a uniform dose to the target volume. A one-dimensional intensity profile from a gantry angle of $\phi = 20^\circ$ is shown [3]. . . . . | 19 |
| 2-4 | Example of dose distributions in IMRT (a,b) and VMAT (c,d) plans for radiotherapy to the prostate and pelvic lymph nodes. The target volume is shown in red. Increased sparing of the rectum and bladder is achieved in the VMAT plan [4]. . . . .                            | 20 |
| 2-5 | Example set of DVHs from a sarcoma treatment plan. Figure modified from [5]. . . . .  | 21 |

|     |  |    |
|-----|--|----|
| 2-6 | This chart shows the partially automated workflow of MCO-informed VMAT planning imagined in this study. The elements that are developed in this study are highlighted in green. This workflow benefits from the efficiency of automation without compromising the personalization of typical treatment planning. . . . .   | 25 |
| 3-1 | This flowchart illustrates each step in the process of generating a VMAT plan with the treatment planning model. The white boxes show each kind of data used in this process, and the blue boxes show operations performed on that data. . . . .   | 29 |
| 4-1 | This box and whisker plot compares the distribution of HI for the test cases planned using the automated planning model and the MCO-IMRT cases of Type A from the knowledge base. The average HI for each set is represented with the $\times$ symbol, and the first and third quartiles and medians are demarcated with horizontal lines. It can be seen that the MCO-IMRT plans have a significantly lower average HI, but that the HI of each test case is within the range of HI for the MCO-IMRT plans. . . . . | 35 |
| 4-2 | This plot displays a selection of DVHs from the MCO-informed VMAT plan for test case 1 (dotted lines) overlaid on the same DVHs from the MCO-IMRT plan for case A-19 in the knowledge base (solid lines). The HI of the PTV for test case 1 is 0.128. The HI of the PTV for A-19 is 0.057. . . . .   | 37 |

# List of Tables

|     |   |    |
|-----|---|----|
| 3.1 | DVH Points Set as Objectives for Minimum and Maximum Dose at Corresponding Percent Volume and Constraints for Global Minimum and Maximum Dose . . . . .       | 30 |
| 4.1 | Final DVH Points Set as Objectives for Minimum and Maximum Dose at Corresponding Percent Volume and Constraints for Global Minimum and Maximum Dose . . . . . | 34 |



# Chapter 1

## Introduction

One of the most obstinate challenges in the effort to develop effective cancer treatments is the selective targeting of cancer cells and sparing of normal ones. Ionizing radiation is a particularly effective agent of cell death relative to other physical, chemical and biological agents because of its ability to inflict irreparable damage to a cell's DNA [6]. Ionizing radiation is used to treat cancer by repeatedly targeting tumor sites with radiation while sparing nearby tissues as much as possible. Over the last fifty years, radiation therapies have improved drastically in their precision targeting of tumor sites. Radiation therapy is now a common and effective treatment for many forms of cancer. However, modern radiation therapy modalities are still being improved through the development of better optimization algorithms, real-time target tracking and patient immobilization techniques.

The name “external beam radiation therapy” encompasses many therapy modalities, but they all involve the exposure of a target volume to one or more beams of radiation, usually produced using some form of accelerator. Intensity-modulated radiation therapy (IMRT) is one of the most common modalities. The primary advantage of IMRT over more primitive photon therapies is its manipulation intersecting high-energy photon beams to deliver a dose distribution that closely conforms to the shape of a tumor [2]. During IMRT, the target volume (comprised of the tumor and

peripheral tissue) is subjected to multiple intersecting, high-energy photon beams of variable intensity. For any given case of IMRT, the number of beams, their angles of incidence on the target, their two-dimensional shape and intensity profile can be collectively optimized to deliver maximal conformity of dose to the target and minimal dose to surrounding organs at risk (OARs) [7].

When creating a treatment plan, physicians face difficult trade-offs between the homogeneity of dose to the target volume and the sparing of OARs. In order to allow physicians to navigate this tradeoff, many clinics create IMRT treatment plans using multi-criteria optimization (MCO). MCO is an algorithm that selects parameters like beam angles, beam intensities and two-dimensional beam shapes in order to optimize a treatment plan according to a set of objectives. Physicians can “toggle” through the relative weightings of these objectives and choose the plan that best fits the needs of a given patient [8]. For example, a particularly young breast cancer patient may be given a relatively conservative treatment plan in the hope of minimizing the risks associated with damage to cardiac tissues.

Volumetric-modulated arc therapy (VMAT) is another modality of external beam radiation therapy, and is the logical progression of IMRT. Instead of using a finite number of beams that intersect in a target volume, VMAT uses beams that rotate about the patient in a continuous arc with the tumor located at its isocenter. The speed of gantry rotation, two-dimensional beam shape and dose rate are all modulated in time as the gantry rotates about the target. With far more degrees of freedom than IMRT, VMAT has the potential to deliver treatments that provide comparable coverage of target volumes and better sparing to OARs [9]. However, the development of MCO-like methods for VMAT has historically proven challenging. For years, many clinics had the capability of delivering VMAT but there existed no robust method of optimizing VMAT treatment plans [10]. MCO-informed VMAT planning was proposed by Chen et al. (2014) as a potential “simpler solution” [10]. MCO-informed VMAT planning relies on first generating an MCO-optimized IMRT plan and then

using dose-volume data from this plan to inform the optimization of the VMAT plan [10]. This study develops a similar technique for MCO-informed VMAT treatment planning for prostate cancers.

The purpose of this study was to construct a model for the automated generation of initial VMAT treatment plans for prostate cancer using a knowledge base of previously implemented MCO-IMRT plans. New cases recommended for VMAT are matched with the most similar historical case treated with MCO-IMRT in the knowledge base. A selection of treatment planning data from that historical case is used to inform the initial optimization of the VMAT treatment plan for the new case. This automated, knowledge-based optimization is intended to serve as a “first pass” that would then be further tuned to the individual patient by a trained treatment planner. This kind of partially automated treatment planning workflow could significantly improve the timeliness of non-MCO VMAT planning.

The final product of this study consists of a completed knowledge base of ninety-six MCO-IMRT plans and the selection of treatment planning data used to inform the automated generation of VMAT treatment plans.





# Chapter 2

## Background

### 2.1 History of Modern Radiation Therapy

Pierre and Marie Curie first isolated the element radium in the year 1898. Within a few years, it was already being used in cancer treatments [11]. Since the discovery of ionizing radiation's ability to damage human tissues, physicists and physicians have developed numerous techniques for selectively targeting cancer cells. Therapies have been delivered using external beams, radioactive “seeds” implanted in the body, and curved plates designed to treat tumors surrounding the delicate tissues of the spinal cord [12].

External beam radiation therapies are one of the most frequently prescribed types of radiation therapy. Since the development of the first medical linear accelerator at Stanford in 1957, external beam radiation therapies have progressed from primitive modalities that relied on stationary beams collimated by simple lead blocks to highly advanced modalities with intricately shaped beams that can rotate 360° about a patient on a wall-mounted gantry [2].

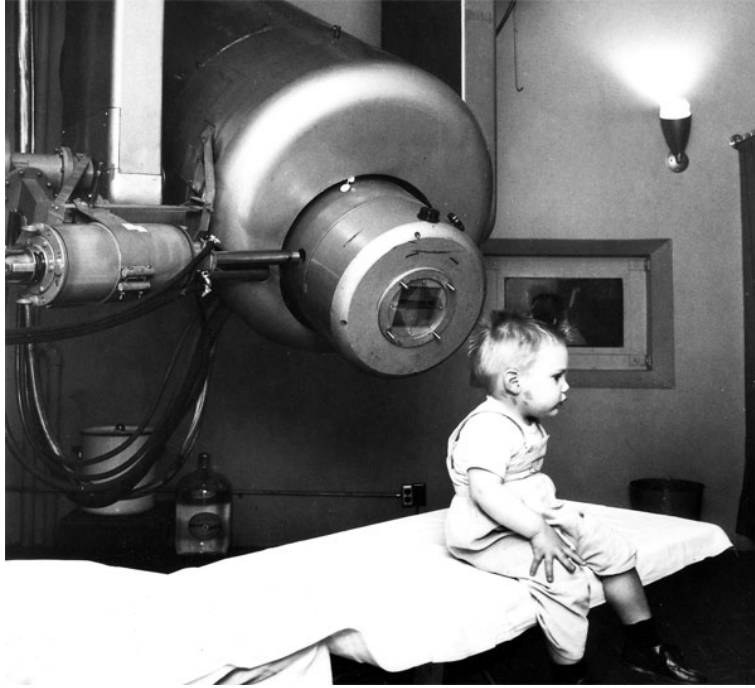


Figure 2-1: The first patient treated with a medical linear accelerator was a two-year-old boy with an ocular tumor [1].

## 2.2 IMRT and VMAT

This study is primarily concerned with two common modalities of external beam radiation therapy: Intensity-Modulated Radiation Therapy (IMRT) and Volumetric-Modulated Arc Therapy (VMAT). During IMRT, the target volume is subject to multiple stationary intersecting beams of high-energy photons. These beams are collimated to conform to the shape of the target volume using a device called a multi-leaf collimator (MLC), shown in Fig. 2-2. Its sliding tungsten leaves can be used both to form the two-dimensional shape of a beam and to shape the beam's two-dimensional intensity profile.

During VMAT, the target volume is also subject to irradiation from many angles. However, the beam does not “turn off” while the gantry rotates as it does in IMRT. Instead, the beam is “on” as the gantry rotates continuously about the patient and the MLC leaves move continuously to shape the beam in both space and intensity.

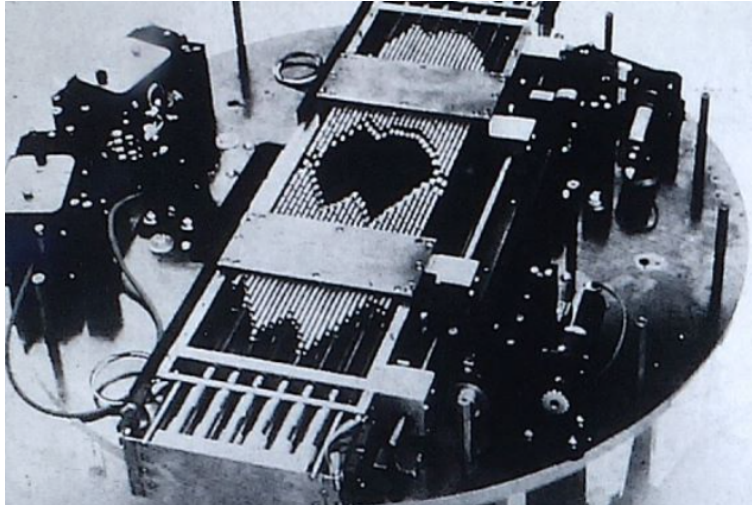


Figure 2-2: A typical MLC consists of 40 pairs of tungsten “leaves” that are independently driven. MLCs are ideal for treatment modalities like IMRT and VMAT that utilize many beam shapes and modulated beam intensity [2].

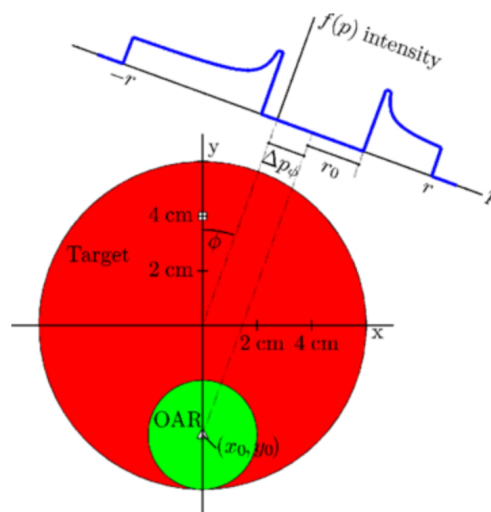


Figure 2-3: Archetypal case of a target volume (red) wrapped around an OAR (green). Simply “blocking” dose from reaching the OAR does not achieve a uniform dose to the target volume. A one-dimensional intensity profile from a gantry angle of  $\phi = 20^\circ$  is shown [3].

VMAT offers the advantage of faster treatment delivery, as well as the potential for the delivery of doses that more closely conform to target volumes and provide better sparing to organs at risk [4].

A comparison of IMRT and VMAT dose distributions for a typical prostate case is shown in Fig. 4-2. The increased conformality of dose to the target and improved dose sparing to surrounding organs at risk are typical results of VMAT planning studies [4].

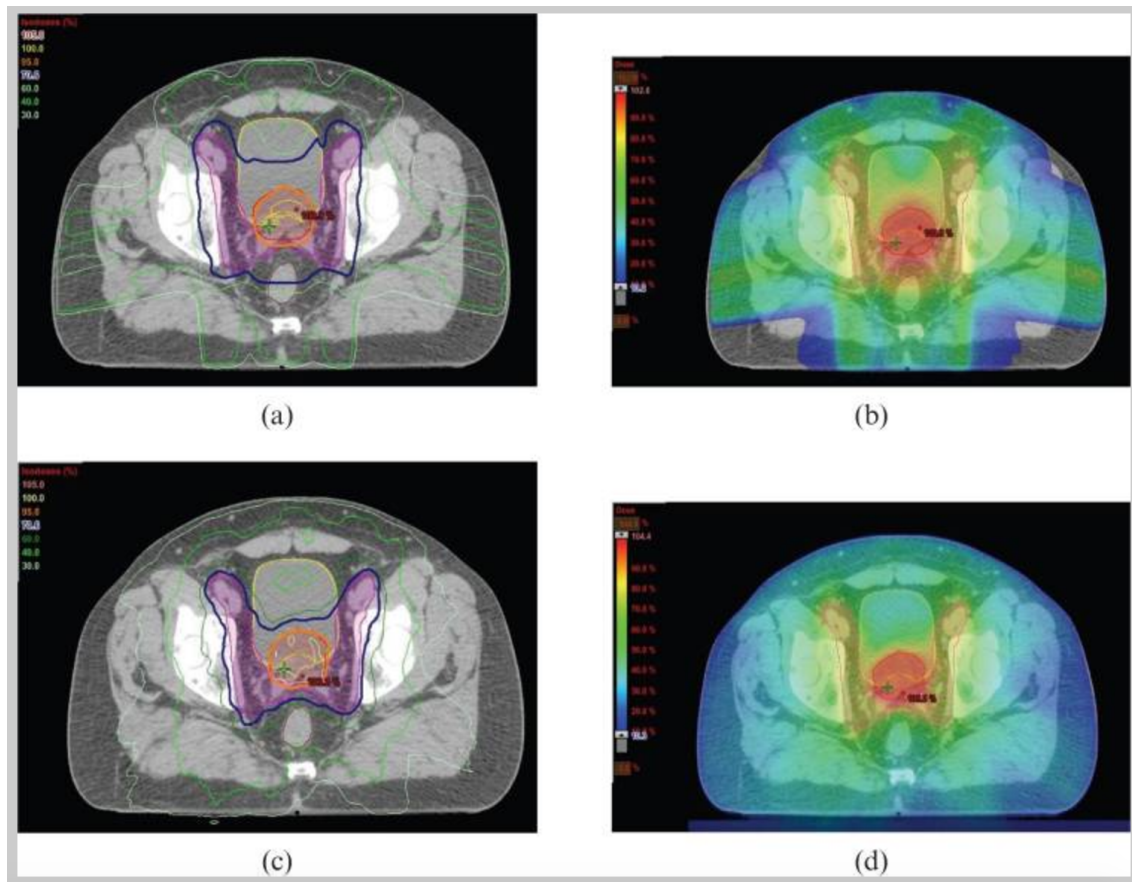


Figure 2-4: Example of dose distributions in IMRT (a,b) and VMAT (c,d) plans for radiotherapy to the prostate and pelvic lymph nodes. The target volume is shown in red. Increased sparing of the rectum and bladder is achieved in the VMAT plan [4].

## 2.3 The Dose-Volume Histogram

While fluence maps like these are useful as they show areas of high and low dose relative to anatomical structures, they are not ideal for quantitatively comparing two treatment plans. This is typically done using dose-volume histograms (DVHs). DVHs can be drawn for any volume that is contoured (outlined in 3-D space) in a CT scan, like the target volume (referred to as the planning treatment volume, or PTV) or any of the OARs. DVHs plot the fraction  $y$  of a given volume that receives a certain dose  $x$  or higher, as a function of dose [2]. DVHs are technically cumulative histograms. Differential dose-volume histograms can also be defined for any volume, but they are rarely used.

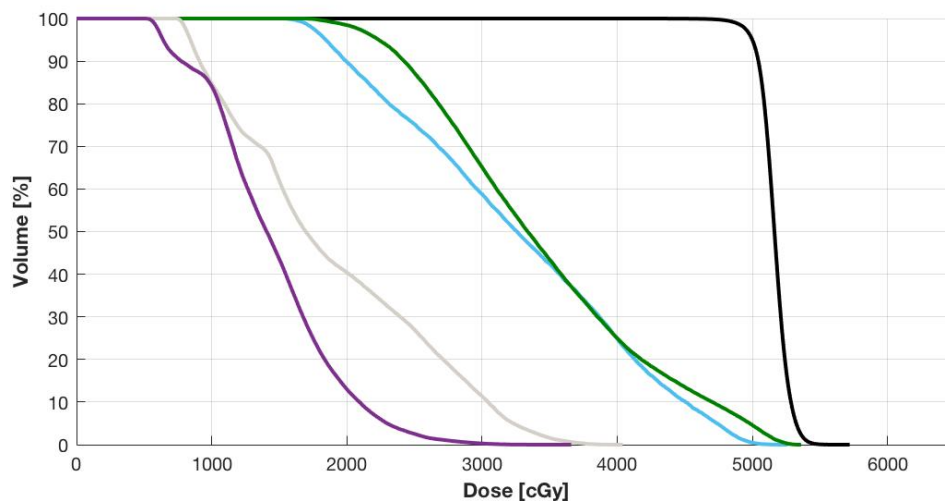


Figure 2-5: Example set of DVHs from a sarcoma treatment plan. Figure modified from [5].

Fig. 2-5 shows an example of a typical set of DVHs for a sarcoma treatment plan. The DVH for the PTV is shown in black. Ideally this curve would form a perfect right angle at  $x = D_{Rx}$ , indicating that 100% of the PTV receives exactly the prescribed dose. This is not physically possible in reality, but most plans do come close. The DVHs for various OARs are shown in color. It can be seen that the OAR shown in purple is better spared than the OAR in green. Ideally, these curves would all be

vertical lines at 0 cGy, indicating that the organ was completely spared. Again, this is not actually possible. However, when a patient’s treatment plan is created it is optimized based on these objectives.

One important quantitative metric used to evaluate treatment plans is the homogeneity index (HI) of the dose to the PTV.

$$HI = (D_2 - D_{98})/D_{Rx} \quad (2.1)$$

where  $D_x$  represents the dose such that  $x\%$  of the PTV volume receives that dose or higher and  $D_{Rx}$  represents the prescription dose [13]. In an ideal treatment plan where the DVH for the PTV is a perfect right angle at  $D_{Rx}$ , HI would be zero. Increasing HI represents increasing heterogeneity of dose to the PTV.

## 2.4 Multi-Criteria Optimization

All of the inputs necessary to deliver a certain fluence map to a three-dimensional volume are referred to as a “treatment plan.” In the case of IMRT, this consists of the number of beams, beam angles, two-dimensional beam shapes, and beam intensity profiles. In the case of VMAT, a treatment plan consists of MLC leaf starting position, as well as gantry angular velocity, MLC leaf velocity and direction, and beam dose rate for all angles. When a treatment plan is created, all of these parameters must be chosen. A handful of physical limits of medical linear accelerators constrain the plans they can deliver. For example, each model of medical linear accelerator has some maximum gantry velocity and maximum MLC leaf velocity. These constraints are taken into account whenever a treatment plan is made.

It is often the case that many slightly different treatment plans would be effective for a given patient and there is no immediately obvious best one. For example, often the DVH for the PTV cannot be improved without degrading the DVHs for several OARs. IMRT treatment plans are created in many clinics using multi-criteria

optimization (MCO), an optimization process that allows physicians to navigate these clinical trade-offs.

A treatment plan is considered Pareto-optimal for a given set of objectives and constraints if there is no other feasible treatment plan that is better in one objective and at least as good in all others. The set of all Pareto-optimal plans for a treatment is called the Pareto surface [8]. In practice, a Pareto surface takes the form of a database of possible treatment plans. A physician can navigate this database to explore planning trade-offs and choose the plan that is most appropriate for their patient [8]. For example, while radiation therapy has been shown to be an effective treatment for early stage breast cancer, it has also been shown to increase risk of ischemic heart disease [14]. If a patient is very young or is known to already be at risk of heart disease, her physician may choose a more conservative treatment plan that sacrifices some homogeneity of tumor coverage in order to minimize dose to the heart. For an older patient, or one who is at less risk of developing heart disease, it might be appropriate to choose a more aggressive treatment plan.

## 2.5 MCO-Informed VMAT

The model implemented in this study uses a knowledge base of treatment planning data from prostate cancer cases historically treated in the MGH clinic. For every case in this knowledge base, CT scans have been used to generate overlapping volume histograms (OVHs). OVHs are a useful tool for quantifying the relative volume and spatial positioning of anatomical structures. In this study, an anatomical similarity metric based on OVHs was used to match new test cases to the most similar historical cases in the knowledge base.

The greater number of degrees of freedom provided by VMAT theoretically allow for plans that are of equal or better quality than IMRT plans for the same case. Thus, treatment planning data drawn from anatomically similar patients treated with IMRT

can be used to provide the a non-MCO optimization algorithm with a viable starting point from which to further optimize. In this study, selection of treatment planning data from historical cases was used to inform the initial optimization of VMAT treatment plans for their respective matched test cases. The specific purpose of this study was to construct the knowledge base of MCO-IMRT plans and to refine the selection of treatment planning data to be used in MCO-informed VMAT optimization.



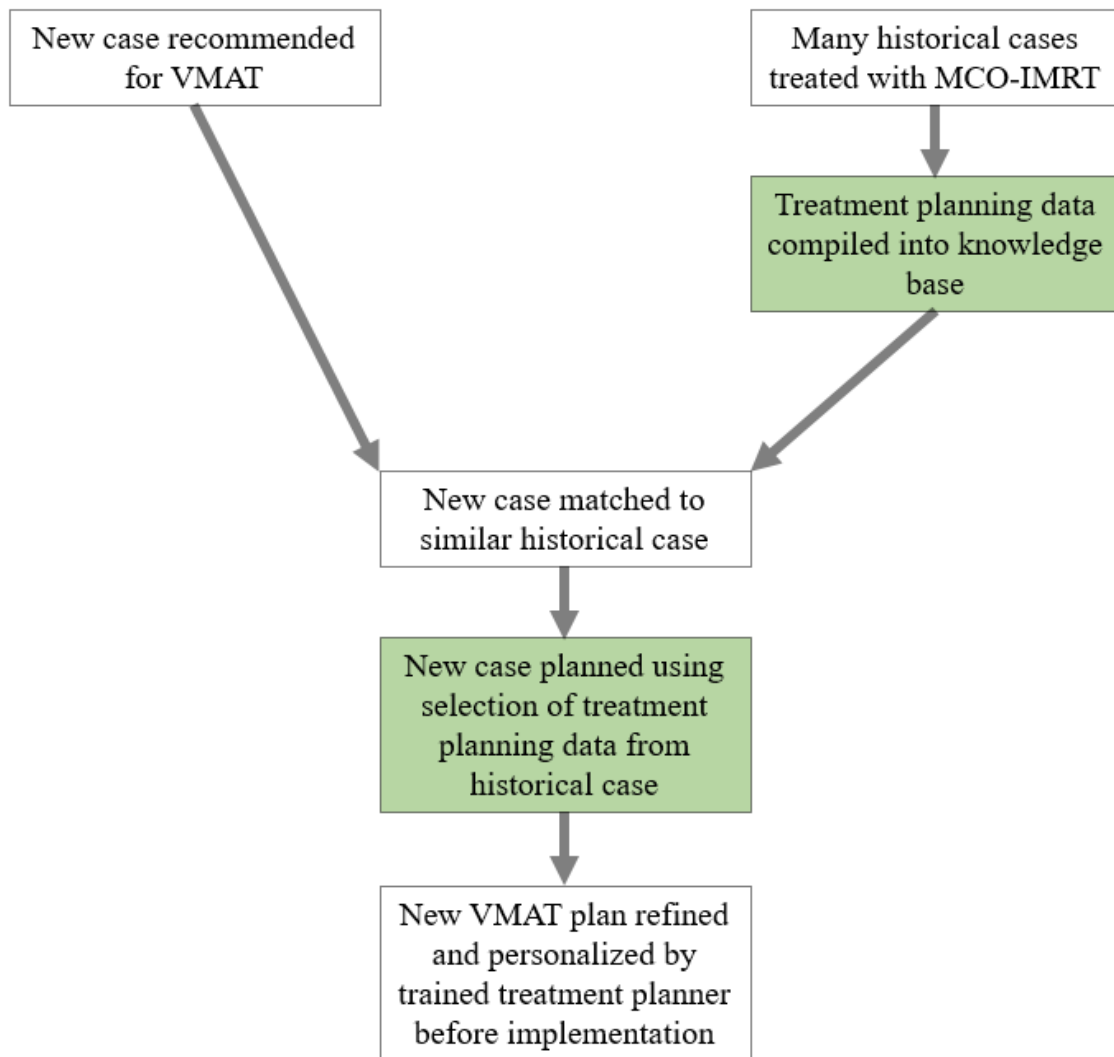


Figure 2-6: This chart shows the partially automated workflow of MCO-informed VMAT planning imagined in this study. The elements that are developed in this study are highlighted in green. This workflow benefits from the efficiency of automation without compromising the personalization of typical treatment planning.



# Chapter 3

## Methods

### 3.1 Patient Cohort

The cohort used in the MCO-IMRT knowledge base consists of 96 patients previously treated for prostate cancer in the MGH clinic. The cohort is made up of three treatment categories: 33 who were treated with IMRT to a PTV in the prostate and seminal vesicles (Type A), 25 who were treated with prostate resection and IMRT with prostate bed PTVs (Type B), and 38 who were treated with prostate resection and IMRT with prostate bed and lymph node PTVs (Type C). The patient data used in this study consisted of contoured CT scans, prescription doses, fractionation schemes and DVHs from each treatment plan. All protected health information was de-identified in accordance with HIPAA “safe harbor” standards [15].

### 3.2 Knowledge Base Construction

The first step in constructing the knowledge base was to identify and discard unnecessary data. Raw patient treatment plan data was exported from the clinic’s treatment planning software (TPS) in the form of detailed DVHs for every structure contoured during treatment planning. Much of this raw data would not be relevant

to informing the treatment planning for a similar future case. While raw TPS DVHs are extremely granular, this knowledge base only calls for 101 points from each DVH—the dose value  $x$  and corresponding 1% volume increment  $y$  from  $y = 0\%$  to  $100\%$ . Raw treatment planning data also contains DVHs for far more contoured volumes, or regions of interest (ROIs), than are relevant for this model. During treatment planning, it is common to contour many subsidiary ROIs within larger ones for the purpose of identifying “hot spots” (small volumes subject to exceptionally high doses). These subsidiary ROIs are not of interest in this study. Only the structures listed in Appendix A were included in the knowledge base.

Using raw treatment planning data also presents the complication of inconsistent terminology. While one treatment planner might label an ROI “LLN” for “left lymph node,” another planner might use the label “Left\_LN” for the same structure. Data cleaning scripts must search DVH labels for all feasible case-sensitive words, phrases or acronyms for each ROI.

In this study, a python script was used to identify all relevant ROIs by key letter groups within their DVH titles and to abbreviate their DVHs to only the 101 points necessary. These refined DVHs were then normalized by prescription dose and organized into banks by treatment type. In this setup, any treatment planning model configured to use DVH data from these treatment plans can draw automatically from this knowledge base.

### 3.3 Model Construction

The model created in this study was designed for and developed using the RayStation (version 2.5, RaySearch Laboratories, Stockholm, Sweden) treatment planning software.

Fig. 3-1 illustrates how a new VMAT plan is actually generated using the model. First, the corresponding IMRT plan is selected from the knowledge base. The model

uses DVH data from this old plan to define the objectives that will be used in the optimization of the VMAT plan for the new patient. RayStation then runs the iterative non-MCO optimization. When the it is finished, the new plan can be viewed. DVHs for all contoured regions in the new patient’s CT scan can be seen, as well as a 3-D dose fluence map of the treatment plan.

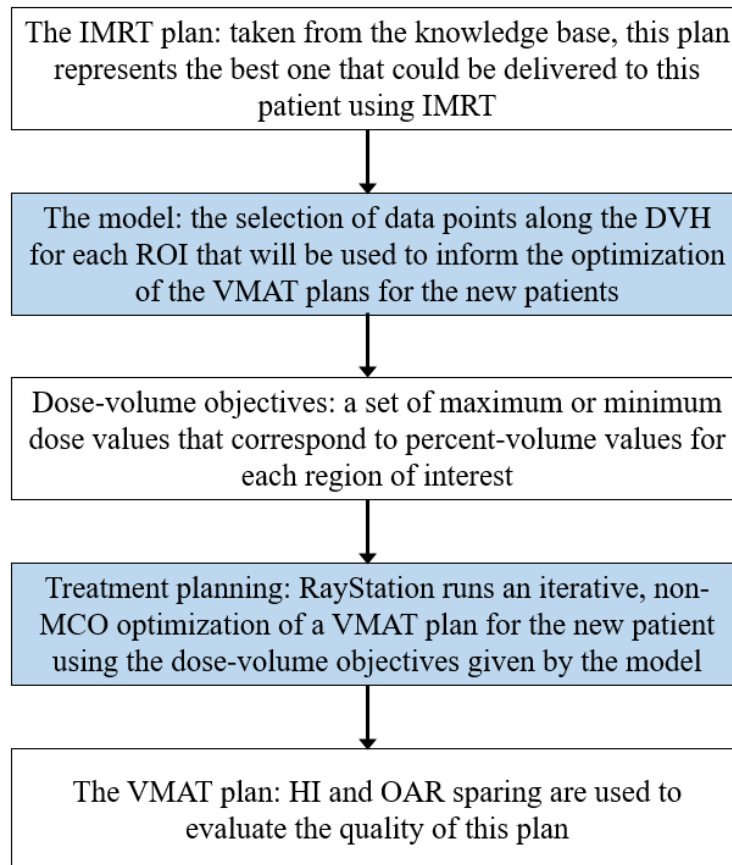


Figure 3-1: This flowchart illustrates each step in the process of generating a VMAT plan with the treatment planning model. The white boxes show each kind of data used in this process, and the blue boxes show operations performed on that data.

The initial selection of DVH data used to create the baseline goals and constraints for optimization was based on tissue dose tolerances, as well as volume intervals selected to give sufficient information to the algorithm to perform a complete optimization. Dose tolerances have been determined empirically by radiation biologists for

most tissues and organs in the human body and can serve as a useful benchmark in treatment planning [11]. DVH points beyond those related to dose tolerances were first included for each ROI at approximately regular intervals from 0% to 100%. This initial selection of DVH points is included in Table 3.1.

Each value  $y$  listed in Table 3.1 represents a %-volume value where a dose-related goal is to be set for a test case in RayStation. For example, The right femur has a maximum dose objective at 8% volume. This means that the dose value corresponding to 8% volume in the DVH for the right femur in the historical case is to be set as the goal for the maximum dose at 8% volume in the plan for the test case.

Table 3.1: DVH Points Set as Objectives for Minimum and Maximum Dose at Corresponding Percent Volume and Constraints for Global Minimum and Maximum Dose

| Region of Interest | Maximum Dose Objectives | Minimum Dose Objectives | Global Maximum Dose Objective | Global Minimum Dose Objective |
|--------------------|-------------------------|-------------------------|-------------------------------|-------------------------------|
| PTV                | 1, 5, 20                | 95, 98, 99              | 0                             | 100                           |
| CTV                | 1, 20                   | 95, 99                  | 0                             | 100                           |
| Bladder            | 12, 17, 25, 46, 58      | --                      | 0                             | --                            |
| L. Femur           | 8                       | --                      | 0                             | --                            |
| R. Femur           | 8                       | --                      | 0                             | --                            |
| Rectum             | 12, 22, 40              | --                      | 0                             | --                            |
| Ant. Rectal Half   | 6, 15, 30, 50           | --                      | --                            | --                            |
| Ant. Rectal Wall   | 6, 15, 30, 50           | --                      | --                            | --                            |

After the initial selection of goals and constraints was made, five test cases of treatment type A were matched to cases within the knowledge base. These test cases were planned using the initial model in RayStation 2.5. Of the three treatment types, Type A was chosen for the initial refinement of the automated planning model as these cases are geometrically simple (they have a single target volume) and prototypical of VMAT treatments for many disease sites.

The model was then iteratively refined based on improvements to the HI of the

PTV and dose sparing to the OARs in these test plans. Each optimization ran for 20 iterations. OAR sparing was primarily improved through the inclusion of more goals closer to 100% volume. It was initially thought that inclusion of this information would not improve the quality of plan results, as these volumes correspond to the lowest doses at the “high end” of OAR DVHs. However, OAR sparing improved across all test cases when more OAR goals were included in this volume range. PTV dose homogeneity was better than expected using the earliest configuration of the model and its improvement was slow. PTV HI was ultimately improved through the matching of maximum and minimum dose objectives near 100% volume. Over the course of iterative model improvement, PTV and OAR improvements began to plateau. The final iteration of the model configuration is included in Table 4.1.

The method of improving the VMAT optimization model described in this section does not constitute a robust optimization. Indeed, the selection of treatment planning data that would make the best basis for optimizing a patient’s non-MCO VMAT treatment would be different for every patient. The model developed in this study produces a workable “first pass” VMAT plan for a new patient based on the MCO-IMRT plan of a similar historical patient. If this model were implemented clinically, a treatment planner would start with this first pass and refine the goals and objectives to shape each new treatment plan to the individual patient. This model is not intended to fully automate treatment planning, but rather to inform its results and improve its timeliness.





# Chapter 4

## Results and Discussion

The purpose of this study was to construct a knowledge base of MCO-IMRT plans and to build a model for the automated planning of MCO-informed VMAT using this knowledge base. The model consists of the selection of DVH data to be used as goals and constraints in non-MCO VMAT optimization.

### 4.1 Knowledge Base

The knowledge base constructed in this study consists of the complete set of uniform dose volume histograms corresponding to all of the regions of interest listed in Appendix A, as well as prescription dose values, fractionation schemes, and professionally contoured clinical CT scans, for ninety-six cases of prostate cancer treated in the MGH clinic. This knowledge base was built from raw treatment planning data exported from the RayStation 2.5 treatment planning system used in the MGH clinic. The kind of knowledge base created in this study has the potential to serve as a useful tool for future studies aimed at comparing the quality of new treatment modalities or optimization methods with the “gold standard” of MCO-IMRT. Growing interest in using deep learning in clinical research will lead to increasing demand for resources like this knowledge base.

## 4.2 Automated Treatment Planning Model

The model constructed in this study allows for automated planning of MCO-informed VMAT based on a knowledge base of previously-implemented MCO-IMRT plans. Rather than using all available DVH data, as has been done in previous studies [10], this simplified model uses only a selection of points that was empirically refined to produce a more streamlined model. The purpose of this model is not to completely automate the work of treatment planners, but rather to provide them with a better “first pass” from which to further optimize when performing the notoriously labor-intensive process of non-MCO VMAT planning. This type of partially automated workflow allows for more time-efficient treatment planning without sacrificing the benefits of treatment personalization.

Table 4.1: Final DVH Points Set as Objectives for Minimum and Maximum Dose at Corresponding Percent Volume and Constraints for Global Minimum and Maximum Dose

| Region of Interest | Maximum Dose Objectives        | Minimum Dose Objectives | Global Maximum Dose Objective | Global Minimum Dose Objective |
|--------------------|--------------------------------|-------------------------|-------------------------------|-------------------------------|
| PTV                | 1, 5, 20, 95                   | 95, 98, 99              | 0                             | 100                           |
| CTV                | 1, 20, 99                      | 95, 99                  | 0                             | 100                           |
| Bladder            | 12, 17, 25, 46, 58, 70, 80, 90 | --                      | 1                             | --                            |
| L. Femur           | 8, 50                          | --                      | 1                             | --                            |
| R. Femur           | 8, 50                          | --                      | 1                             | --                            |
| Rectum             | 12, 22, 40, 70, 80, 90         | --                      | 1                             | --                            |
| Ant. Rectal Half   | 6, 15, 30, 50, 70, 80, 90      | --                      | --                            | --                            |
| Ant. Rectal Wall   | 6, 15, 30, 50, 70, 80, 90      | --                      | --                            | --                            |

The final set of volumes used to define the goals and constraints included in the model are listed in Table 4.1. The global maximum dose objectives for several OARs are set to 1%. This means that the dose received by only the highest-dosed 1% of the

voxels in that volume in the historical case is set as the absolute dose ceiling for that volume in the test case.

The test cases planned using this model demonstrated an average HI of  $0.245 \pm 0.080$ . For comparison, the average HI of MCO-IMRT plans of Type A in the knowledge base is  $0.093 \pm 0.073$ . Thus, the VMAT plans show a 163% increase in HI on average, compared to the MCO-IMRT plans. This indicates that the plans produced using the automated treatment planning model are worse on average than the MCO-IMRT plans in the knowledge base on the metric of PTV dose homogeneity.

However, Fig. 4-1 shows that the absolute range of HI of the model-generated plans is within the range of HI of plans of Type A in the knowledge base. This means that while the model produces VMAT plans with worse average PTV dose homogeneity than the original IMRT plans, they are all within a clinically acceptable range.

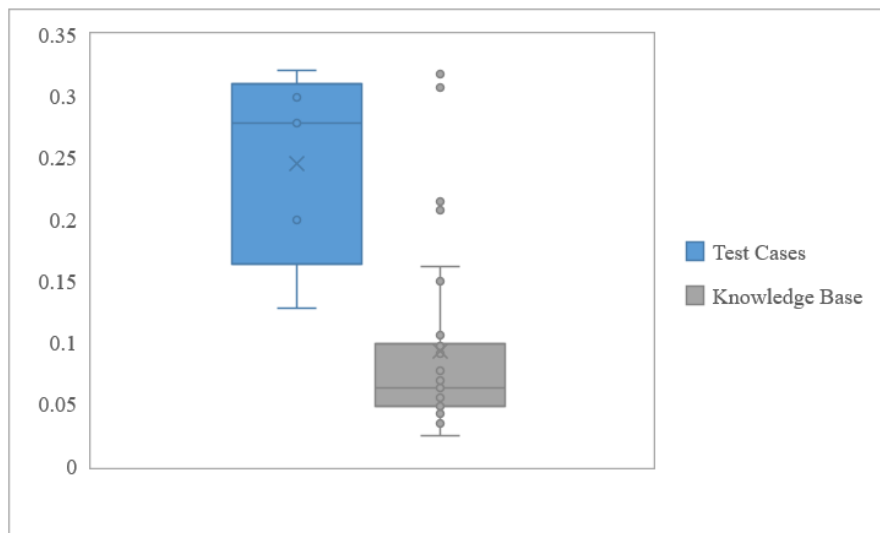


Figure 4-1: This box and whisker plot compares the distribution of HI for the test cases planned using the automated planning model and the MCO-IMRT cases of Type A from the knowledge base. The average HI for each set is represented with the  $\times$  symbol, and the first and third quartiles and medians are demarcated with horizontal lines. It can be seen that the MCO-IMRT plans have a significantly lower average HI, but that the HI of each test case is within the range of HI for the MCO-IMRT plans.

These auto-generated plans are clearly not adequate for implementation without further improvement. However, the model is intended to automate the generation of “first pass” treatment plans with no personalization. As a result, the HI range of these test cases is promising. Treatment planners can use these “first pass” plans to much more quickly shape a patient’s final, high-quality personalized treatment plan than if they were starting from scratch.

Fig. 4-2 is included as an example of DVH data from a VMAT plan generated by the model overlaid with the DVH data from its matched IMRT plan from the knowledge base. The figure shows the DVHs from the MCO-IMRT plan for case A-19 in the knowledge base as solid lines. It shows the DVHs from the VMAT plan generated by the model for test case 1 as dotted lines. This figure can be used to compare the relative dose sparing to OARs and the relative homogeneity of target coverage. The VMAT plan provides better sparing to the rectum and to the left and right femur. The IMRT plan provides slightly better sparing to the bladder. The decreased homogeneity of dose to the target in the VMAT plan can be seen in the relative slopes of the solid and dotted PTV and prostate curves. However, in general these DVH sets are visibly similar. While it stands to be significantly improved from this initial, auto-generated version, the VMAT plan for test case 1 is a very good place for a treatment planner to start an optimization.

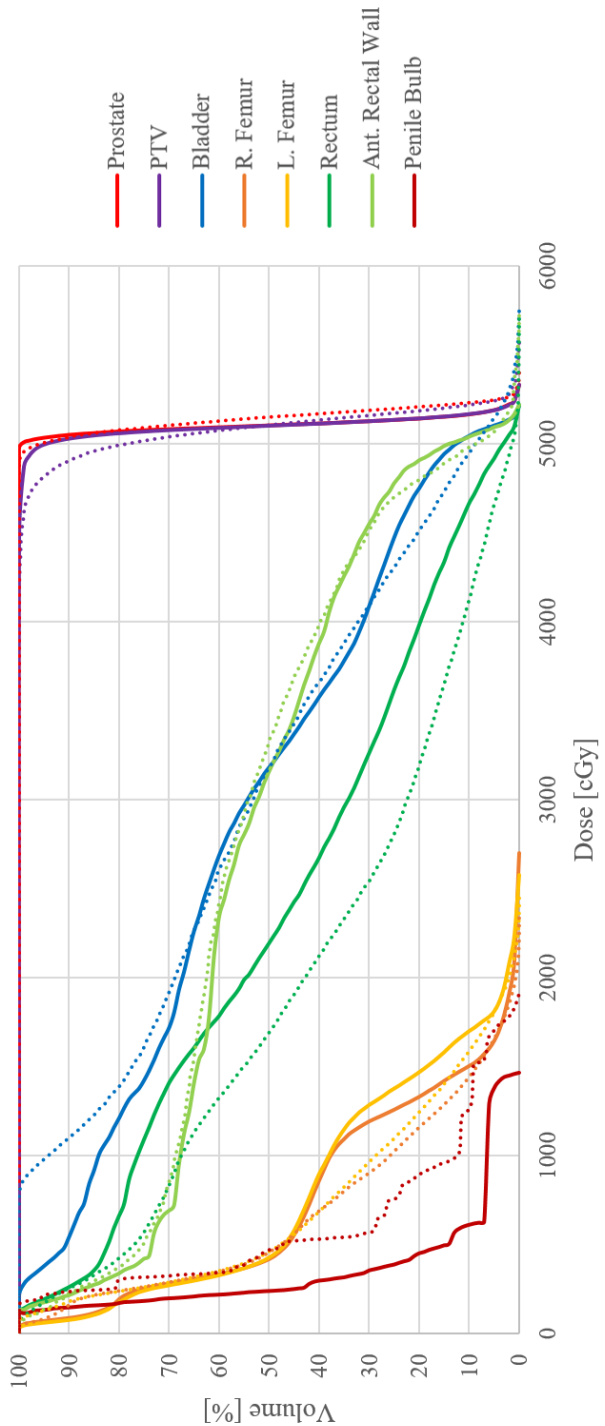


Figure 4-2: This plot displays a selection of DVHs from the MCO-informed VMAT plan for test case 1 (dotted lines) overlaid on the same DVHs from the MCO-IMRT plan for case A-19 in the knowledge base (solid lines). The HI of the PTV for test case 1 is 0.128. The HI of the PTV for A-19 is 0.057.

### 4.3 Limitations of this Study

The results of the automated planning model produced in this study can always be improved by increasing the number and diversity of cases in the knowledge base. The model produces its best results when new cases are matched with very similar historical ones. When a new case is matched with a truly identical historical case, the MCO-IMRT plan represents the truly ideal starting point for the new patient's VMAT optimization [10]. If a model like the one produced in this study were to be implemented clinically, its knowledge base would need to be vast.

The model produced by this study would also have to be improved significantly before clinical implementation. Far more test cases of treatment Type A would need to be run to refine the model for that treatment type. Completing a project of this computational scale would require the use of many machines running optimizations in parallel. Consideration might be given to the potential weighting of the results of different test cases based on how typical they are of their treatment type. Variations of the model would also have to be produced for treatment Types B and C.

# Chapter 5

## Conclusion

Radiation therapies have advanced drastically over the last fifty years. However, they are still being improved through the development of more advanced optimization algorithms, real-time target tracking and patient immobilization techniques. The development of multi-criteria optimization represents an important recent advance of the art and science of radiation therapy planning. MCO-IMRT is now the “gold standard” of radiation therapy against which new modalities are measured.

VMAT, the logical progression of IMRT, has the possibility to deliver comparable dose coverage to target volumes with improved OAR sparing. However, early versions of MCO were not compatible with VMAT. While many clinics were equipped to deliver VMAT, robust methods for its optimization had not yet been developed. Although robust MCO methods for VMAT have been developed since the commencement of this study, it is likely that there will someday be another case where our ability to deliver advanced therapies outstrips our ability to optimize them. In those future cases, knowledge-based treatment planning can serve to bridge that gap while optimization methods are developed.

The purpose of this study was to construct a model for the automated generation of MCO-informed VMAT treatment plans using a knowledge base of previously implemented MCO-IMRT plans. The cohort used in the knowledge base consists of

ninety-six patients previously treated for prostate cancer in the MGH clinic. Cases in the cohort each received one of three common types of treatment for prostate cancer. The patient data used in this study consisted of contoured CT scans, prescription doses, fractionation schemes and reformatted DVHs from each treatment plan.

Five test cases were matched to historical cases within this knowledge base using a metric for anatomical similarity that was developed in previous work at MGH. An initial model was constructed for the automated generation of new MCO-informed VMAT plans based on the treatment planning data from their matched MCO-IMRT plans. This model consists of the selection of treatment planning data used as objectives for maximum and minimum dose to certain fractional volumes, and global maximum and minimum doses to certain volumes. The model was iteratively refined based on PTV homogeneity and OAR sparing. The final model produced MCO-informed VMAT plans with an average HI of  $0.245 \pm 0.080$ . Compared to the average HI of the MCO-IMRT plans of  $0.093 \pm 0.073$ , these auto-generated plans represent a reasonable starting place for refinement by a trained treatment planner.

Future work on the automated planning model should include the refinement of the model based on more test cases of treatment type A, as well as the development of similar models for treatment types B and C. Before these knowledge-based models can be integrated into clinical workflow, it is necessary to evaluate the limits of the anatomical similarity metric used to match new cases to historical ones. Given a large enough knowledge base, most new cases will have a sufficiently similar historical case in the knowledge base to usefully inform their treatment plan. However, for new cases that are extreme outliers and are not well-represented by any case in the knowledge base, this kind of model may be of limited practical utility.

Finally, in addition to prostate cancers there are other disease sites that could be candidates for automated planning models like this one. Given the success of VMAT for prostate cancers, there has been some interest in implementing it for other pelvic malignancies such as lower gastrointestinal and gynecological cancers.



Planning studies have shown promising results for cervical cancers in particular [4]. Cervical cancers, like prostate cancers, would provide a promising site for automated knowledge-based planning due to their relative distance from critical OARs.

Automated treatment planning models like this one have the potential to improve the timeliness of laborious treatment planning processes. Developing the science of knowledge-based treatment planning can prepare the field of medical physics to handle future cases where complex radiation therapies can be delivered physically, but cannot yet be optimized computationally. Leaning on the resource of historical clinical data can help us to deliver the best possible therapies in these cases.



# Appendix A

## Regions of Interest

**Type A:** PTV, CTV, prostate, bladder, penile bulb, seminal vesicles, r. femur, l. femur, rectum, ant. rectal half, post. rectal half, ant. rectal wall, post. rectal wall

**Type B:** PTV, CTV, prostate bed, bladder, penile bulb, seminal vesicles, r. femur, l. femur, small bowel, large bowel, rectum, ant. rectal half, post. rectal half, ant. rectal wall, post. rectal wall

**Type C:** PTV, PTV total, r. lymph node PTV, l. lymph node PTV, prostate bed, bladder, penile bulb, seminal vesicles, r. femur, l. femur, r. lymph node, l. lymph node, small bowel, large bowel, rectum, ant. rectal half, post. rectal half, ant. rectal wall, post. rectal wall



# Appendix B

## DVH Data Cleaning Script

```
import os
filenames=[]
for item in os.listdir('DVH text files/'):
    filename=item
    if '.dvh' in filename:
        if '-1' not in filename:
            filenames.append(filename)
for filename in filenames:
    file=open('DVH text files/' + filename, 'r')
    lines = file.readlines()
    #remove .dvh from end of filename
    filename=filename[:-4]
    #list of key terms in ROI names of interest
    ROI_terms=['PTV', 'ptv', 'CTV', 'ctv', 'Pros', 'pros', 'Blad',
               'blad', 'Fem', 'fem', 'sem', 'Sem', 'ves', 'Ves',
               'Rect', 'rect', 'Penile', 'penile', 'Bulb', 'bulb',
               'RLN', 'rln', 'LLN', 'lln', 'Bowel', 'bowel', 'Node',
               'node', 'Pelvic', 'pelvic']
```

```

#recurring structures we're not interested in
bad_terms=['PTV 5040 Wall', 'PTV 7920 Wall', 'R+L Femur']

ROIs = []

#start of DVH data following ROI name
starters = []

Allregions=[]
Rejected_regions=[]

#iterate through lines, get patient number and ROIs
i=0
for line in lines:
    if 'PatientNumber' in line:
        #pulls just patient's number
        patient_number=line[13:-1]

    if 'RoiName' in line:
        r=line[9:-1]
        Allregions.append(r)
        if r not in bad_terms:
            for term in ROI_terms:
                if term in line:
                    ROIs.append(line[9:-1])
                    starters.append(i+3)
                    break

        i+=1

#Make sure you're not throwing away anything of interest
for thing in Allregions:
    if thing not in ROIs:
        Rejected_regions.append(thing)

```

```

        #print('DISCARDING ' + thing)
##    print(patient_number)
##    print(lines[2])
##    print(Rejected_regions)
##    print('')
##    print(ROIs)
##    print('')
##    print('')
patient_values=[]
patient_DVHs=[]
#go through stuff following ROI names, cut out DVH values
for i in range(len(ROIs)):
    firstline = starters[i]
    values= []
    for j in range(1000):
        line = lines[firstline+j]
        if line == '\n':
            break
        else:
            #values gives data assoc'd with ROI
            values.append(line[0:-1].split('\t'))
#compiles all uncleaned data for structures of interest for
#patient
patient_values.append(values)
#go through values, keep only stuff we want, stick it in
#DVH
DVH=[[ '0.000', '100.000']]
hundreds=[]

```

```

for j in range(len(values)):
    if values[j][1]=='100.000':
        hundreds.append(values[j])
    if values[j][1]=='0.000':
        DVH.append(values[j])
        break
    elif '.000' in values[j][1]:
        DVH.append(values[j])
#DVH will contain only whole percent values from last
#100 to first 0
for k in range(len(hundreds)-1):
    DVH.remove(hundreds[k])
#compile all cleaned DVHs for structures of interest
#for patient
#remove smaller of any duplicate dose values
for j in range(len(DVH)-3):
    if DVH[j][1]==DVH[j-1][1] and DVH[j][1]!='100.000':
        DVH.remove(DVH[j])
for j in range(len(DVH)):
    DVH[j]=float(DVH[j][0])
#convert DVH from list to array
patient_DVHs.append(DVH)
x=len(ROIs)
for i in range(x):
    ROIs.insert(2*i+1, '')
empty=[]
for i in range(102):
    empty.append('')

```



```
x=len(patient_DVHs)
for i in range(x):
    patient_DVHs.insert(2*i+1,empty)
#put patient's DVHs and ROIs into .csv
import csv
with open('csv files/' + filename + '.csv', 'w', newline='') as f:
    writer = csv.writer(f, dialect='excel')
    writer.writerow([ROIs])
    #zip writes DVHs as columns under corresponding ROI names
    writer.writerow(zip(*patient_DVHs))
```



# Bibliography

- [1] M. Baker. Medical linear accelerator celebrates 50 years of treating cancer. Stanford News. <http://news.stanford.edu/news/2007/april18/med-accelerator-041807.html>, 2007. Accessed April 21, 2017.
- [2] F. M. Khan. *The Physics of Radiation Therapy*. Philadelphia: Lippincott Williams & Wilkins, 2010. 9780781788564. pp. 246, 423, 435.
- [3] T. Bortfeld and S. Webb. Single-arc imrt? *Physics in Medicine and Biology*, 54(1):9–20, 2008.
- [4] M. Teoh, C. H. Clark, K. Wood, S. Whitaker, and A. Nisbet. Volumetric modulated arc therapy: a review of current literature and clinical use in practice. *The British Journal of Radiology*, 1007(84):967–996, 2011.
- [5] M. R. Young, D. L. Craft, C. M. Colbert, K. Remillard, L. Vanbenthuisen, and Y. Wang. Volumetric-modulated arc therapy using multicriteria optimization for body and extremity sarcoma. *Journal of Applied Clinical Medical Physics*, 17(6):283–291, 2013.
- [6] E. L. Alpen. *Radiation biophysics*. San Diego: Academic Press, 1998. 0120530856. pp. 123.
- [7] D. Craft and C. Richter. Deliverable navigation for multicriteria step and shoot imrt treatment planning. *Physics in Medicine and Biology*, 58(1):87–103, 2013.

- [8] D. Craft, T. Halabi, H. Shih, and T. Bortfeld. An approach for practical multi-objective imrt treatment planning. *International Journal of Radiation Oncology: Biology, Physics*, 69(5):1600–1607, 2007.
- [9] M. Rao, W. Yang, F. Chen, K. Sheng, J. Ye, V. Mehta, D. Shepard, and D. Cao. Comparison of elekta vmat with helical tomotherapy and fixed field imrt: Plan quality, delivery efficiency and accuracy. *Medical Physics*, 37(3):1350–1359, 2010.
- [10] H. Chen, D. L. Craft, and D. P. Gierga. Multicriteria optimization informed vmat planning. *Medical Dosimetry*, 39:64–73, 2014.
- [11] E. J. Hall and A. J. Giaccia. *Radiobiology for the Radiologist*. Philadelphia: Wolters Kluwer Health, Lippincott Williams & Wilkins, 2012. 9781608311934. pp. 3, 328.
- [12] T. F. DeLaney, G. T. Chen, T. C. Mauceri, J. J. Munro III, F. J. Hornicek, F. X. Pedlow, H. D. Suit, and D. Phil. Intraoperative dural irradiation by customized  $^{192}\text{Ir}$  and  $^{90}\text{Y}$  brachytherapy plaques. *International Journal of Radiation Oncology: Biology, Physics*, 57(1):239 – 245, 2003.
- [13] T. Kataria, K. Sharma, V. Subramani, K. P. Karrthick, and S. Bisht. Homogeneity index: An objective tool for assessment of conformal radiation treatments. *Medical Physics*, 37(4):207–213, 2012.
- [14] S. C. Darby, M. Ewertz, P. McGale, A. M. Bennet, U. Blom-Goldman, D. Bronnum, C. Correa, D. Cutter, G. Gagliardi, B. Gigante, M. Jensen, A. Nisbet, R. Peto, K. Rahimi, C. Taylor, and P. Hall. Risk of ischemic heart disease in women after radiotherapy for breast cancer. *New England Journal of Medicine*, 368(11):987–998, 2013.
- [15] U.S. Department of Health and Human Services. Guidance regarding methods for de-identification of protected health information in accordance

with the health insurance portability and accountability act (hipaa) privacy rule. <https://www.hhs.gov/hipaa/for-professionals/privacy/special-topics/de-identification/standard>, 2007. Section 1.4. Accessed April 26, 2017.